ORIGINAL ARTICLE

Journal of Cachexia, Sarcopenia and Muscle (2021)
Published online in Wiley Online Library (wileyonlinelibrary.com) **DOI:** 10.1002/jcsm.12744

Targeting interleukin-1 for reversing fat browning and muscle wasting in infantile nephropathic cystinosis

Wai W. Cheung[1†], Sheng Hao[2†], Ronghao Zheng[3], Zhen Wang[4], Alex Gonzalez[1], Ping Zhou[5], Hal M. Hoffman[6] & Robert H. Mak[1*]

[1]*Division of Pediatric Nephrology, Department of Pediatrics, Rady Children's Hospital San Diego, University of California, San Diego, La Jolla, CA, USA;* [2]*Department of Nephrology and Rheumatology, Shanghai Children's Hospital, Shanghai Jiao Tong University, Shanghai, China;* [3]*Department of Pediatric Nephrology, Rheumatology, and Immunology, Maternal and Child Health Hospital of Hubei Province, Tongji Medical College, Huazhong University of Science and Technology, Wuhan, China;* [4]*Department of Pediatrics, Shanghai General Hospital, Shanghai Jiao Tong University, Shanghai, China;* [5]*Sichuan Provincial Hospital for Women and Children, Affiliated Women and Children's Hospital of Chengdu Medical College, Chengdu, China;* [6]*Department of Pediatrics, University of California, San Diego, La Jolla, CA, USA*

Abstract

Background *Ctns*$^{-/-}$ mice, a mouse model of infantile nephropathic cystinosis, exhibit hypermetabolism with adipose tissue browning and profound muscle wasting. Inflammatory cytokines such as interleukin (IL)-1 trigger inflammatory cascades and may be an important cause for cachexia. We employed genetic and pharmacological approaches to investigate the effects of IL-1 blockade in *Ctns*$^{-/-}$ mice.

Methods We generated *Ctns*$^{-/-}$ *Il1β*$^{-/-}$ mice, and we treated *Ctns*$^{-/-}$ and wild-type control mice with IL-1 receptor antagonist, anakinra (2.5 mg/kg/day, IP) or saline as vehicle for 6 weeks. In each of these mouse lines, we characterized the cachexia phenotype consisting of anorexia, loss of weight, fat mass and lean mass, elevation of metabolic rate, and reduced *in vivo* muscle function (rotarod activity and grip strength). We quantitated energy homeostasis by measuring the protein content of uncoupling proteins (UCPs) and adenosine triphosphate in adipose tissue and skeletal muscle. We measured skeletal muscle fiber area and intramuscular fatty infiltration. We also studied expression of molecules regulating adipose tissue browning and muscle mass metabolism. Finally, we evaluated the impact of anakinra on the muscle transcriptome in *Ctns*$^{-/-}$ mice.

Results Skeletal muscle expression of IL-1β was significantly elevated in *Ctns*$^{-/-}$ mice relative to wild-type control mice. Cachexia was completely normalized in *Ctns*$^{-/-}$ *Il1β*$^{-/-}$ mice relative to *Ctns*$^{-/-}$ mice. We showed that anakinra attenuated the cachexia phenotype in *Ctns*$^{-/-}$ mice. Anakinra normalized UCPs and adenosine triphosphate content of adipose tissue and muscle in *Ctns*$^{-/-}$ mice. Anakinra attenuated aberrant expression of beige adipose cell biomarkers (UCP-1, CD137, Tmem26, and Tbx1) and molecules implicated in adipocyte tissue browning (Cox2/Pgf2α, Tlr2, Myd88, and Traf6) in inguinal white adipose tissue in *Ctns*$^{-/-}$ mice. Moreover, anakinra normalized gastrocnemius weight and fiber size and attenuated muscle fat infiltration in *Ctns*$^{-/-}$ mice. This was accompanied by correction of the increased muscle wasting signalling pathways (increased protein content of ERK1/2, JNK, p38 MAPK, and nuclear factor-κB p65 and mRNA expression of Atrogin-1 and Myostatin) and the decreased myogenesis process (decreased mRNA expression of MyoD and Myogenin) in the gastrocnemius muscle of *Ctns*$^{-/-}$ mice. Previously, we identified the top 20 differentially expressed skeletal muscle genes in *Ctns*$^{-/-}$ mice by RNAseq. Aberrant expression of these 20 genes have been implicated in muscle wasting, increased energy expenditure, and lipolysis. We showed that anakinra attenuated 12 of those top 20 differentially expressed muscle genes in *Ctns*$^{-/-}$ mice.

Conclusions Anakinra may provide a targeted novel therapy for patients with infantile nephropathic cystinosis.

Keywords Infantile nephropathic cystinosis; IL-1; Cachexia; Adipose tissue browning; Muscle wasting

Received: 15 January 2021; Revised: 5 May 2021; Accepted: 8 June 2021
**Correspondence to: Robert H. Mak, Division of Pediatric Nephrology, Department of Pediatrics, Rady Children's Hospital San Diego, University of California, San Diego, 9500 Gilman Drive, MC 0831, La Jolla, CA 92093-0831, USA. Phone: 858-822-6717; Fax: 858-822-6776. Email: romak@health.ucsd.edu*
†These authors contributed equally to this work.

Introduction

Cystinosis is a genetic disorder characterized by the accumulation of cystine in different tissues and organs. Infantile nephropathic cystinosis (INC) is the most common and severe form of cystinosis.[1] INC patients exhibit signs and symptoms of the renal Fanconi syndrome and chronic kidney disease (CKD) in early childhood.[2] Metabolic abnormalities such as cachexia are common complications in patients with INC, which are associated with poor quality of life and mortality, and for which there is no current therapy increased expression of inflammatory cytokines, including interleukin (IL)-1β, has been implicated in the aetiology of cachexia and muscle wasting associated with different disease processes. Consistent with this finding, patients with cystinosis had higher concentrations of circulating IL-1β compared with controls.[1] Peripheral blood mononuclear cells from patients with cystinosis revealed a significant increase in IL-1β transcript levels compared with controls.[3] Recent evidence in preclinical models suggested that blockade of IL-1 signalling may be a logical therapeutic target for chronic disease-associated muscle wasting because IL-1β activates nuclear factor-κB (NF-κB) signalling and induces expression of muscle catabolic gene IL-6 and atrogin-1 in C2C12 myocytes.[4,5] Anakinra is an IL-1 receptor antagonist that blocks both IL-1α and IL-1β.[6] Duchenne muscular dystrophy is an X-linked muscle disease characterized by muscle inflammation that is associated with increased circulating serum levels of IL-1β. Subcutaneous administration of anakinra normalized muscle function in a mouse model of Duchenne muscular dystrophy.[7] Similarly, serum IL-1β is elevated in haemodialysis patients, and a 4 week treatment with anakinra was shown to be safe in these patients while significantly reducing markers of systemic inflammation such as C-reactive protein (CRP) and IL-6.[8] In this study, we utilized *Ctns*$^{-/-}$ mice as an established model of INC in which we have previously shown hypermetabolism with adipose tissue browning and profound muscle wasting by 12 months of age.[9] We explored the role of inflammatory cytokines in *Ctns*$^{-/-}$ mice and evaluated the efficacy of IL-1 targeted therapy on adipose tissue browning and muscle wasting. Anakinra was FDA approved for the treatment of rheumatoid arthritis in 2001 and is safe and an effective therapeutic option in a variety of diseases including diseases involving muscle. It may be repurposed as novel therapy for cachexia in INC.

Methods

Study design

All animal work was conducted in compliance and approved by the Institutional Animal Care and Use Committee at the University of California, San Diego. Wild-type (WT), *Il6*$^{-/-}$ and *Il1β*$^{-/-}$, *Ctns*$^{-/-}$, *Ctns*$^{-/-}$ *Il6*$^{-/-}$, and *Ctns*$^{-/-}$ *Il1β*$^{-/-}$ mice were on the same c57BL/6 genetic background. *Ctns*$^{-/-}$ mice were kindly provided by Professor Corinne Antignac, and *Ctns*$^{-/-}$ *Il6*$^{-/-}$ and *Ctns*$^{-/-}$ *Il1β*$^{-/-}$ mice were generated by crossing *Ctns*$^{-/-}$ mice with *Il6*$^{-/-}$ and *Il1β*$^{-/-}$ mice, respectively. Twelve-month-old male mice were used for all of the following five studies. Study 1: We evaluated the gastrocnemius muscle IL-1β and IL-6 mRNA and protein content in *Ctns*$^{-/-}$ mice and WT mice. Results were presented in *Figure* 1A–1D. Study 2: We evaluated the effects of genetic deletion of *Il1β* and *Il6* in *Ctns*$^{-/-}$ mice. We compared *ad libitum* food intake and weight change in WT, *Ctns*$^{-/-}$, *Ctns*$^{-/-}$ *Il6*$^{-/-}$, and *Ctns*$^{-/-}$ *Il1β*$^{-/-}$ mice. The study period was 6 weeks. Results were shown in *Figure* 1E and 1F. Study 3: We evaluated the beneficial effects of genetic deletion of *Il1β* and *Il6* in *Ctns*$^{-/-}$ mice beyond nutritional effects by employing a pair-feeding strategy. The study period was 6 weeks. *Ctns*$^{-/-}$ mice were fed *ad libitum*, and then WT, *Ctns*$^{-/-}$ *Il6*$^{-/-}$, and *Ctns*$^{-/-}$ *Il1β*$^{-/-}$ mice were fed the same amount of rodent diet based on the recorded food intake of *Ctns*$^{-/-}$ mice. Results were shown in *Figure* 1G–1N. Study 4: We evaluated the effects of anakinra in *Ctns*$^{-/-}$ mice. WT and *Ctns*$^{-/-}$ mice were given anakinra (2.5 mg/kg/day, IP) or vehicle (normal saline), respectively. The study period was 6 weeks. All mice were fed *ad libitum*. We compared food intake and weight change in all groups of mice. Results were shown in *Figure* 2A and 2B. Study 5: We evaluated the metabolic effects of anakinra in *Ctns*$^{-/-}$ mice beyond nutritional stimulation by employing a pair-feeding strategy. WT and *Ctns*$^{-/-}$ mice were given anakinra (2.5 mg/kg/day, IP) or vehicle (normal saline), respectively. The study period was 6 weeks. Vehicle-treated *Ctns*$^{-/-}$ mice were fed *ad libitum* while all other groups of mice were fed the same amount of rodent diet based on the recorded food intake of vehicle-treated *Ctns*$^{-/-}$ mice. Results were shown in Figures 2E–2G and 3–6 as well as Supporting Information, *Figures* S1 and S2.

Serum and blood chemistry

Blood urea nitrogen and serum concentration of bicarbonate was measured (*Table* S1). Serum creatinine was analysed by liquid chromatography-tandem mass spectrometry method.[10]

Body composition, metabolic rate, and in vivo muscle function

Body composition (for lean and fat content) of mice was measured by quantitative magnetic resonance analysis

DOI: 10.1002/jcsm.12744

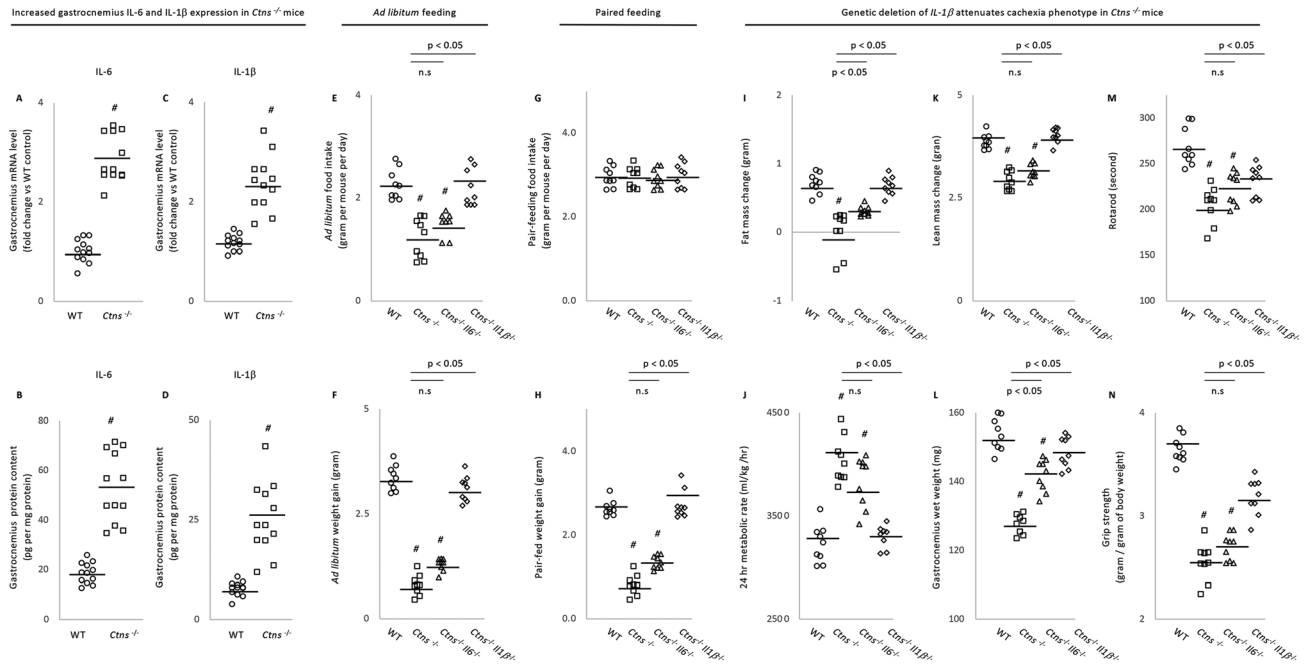

Figure 1 Increased muscle mRNA and protein content of IL-6 and IL-1β in *Ctns*$^{-/-}$ mice and genetic depletion of *Il1β* provides a better rescue of cachexia in *Ctns*$^{-/-}$ mice compared with *Il6* deficiency. Results of three different experiments were shown. For the first study, we compared gene expression and protein content of IL-6 and IL-1β in gastrocnemius muscle in 12-month-old *Ctns*$^{-/-}$ and WT mice. Data were expressed as mean ± SEM. Results of *Ctns*$^{-/-}$ mice were compared with WT mice (*A–D*). For the second study, we compared the metabolic effects of genetic deletion of *Il6* and *Il1β* in *Ctns*$^{-/-}$ mice. Four groups of mice were included, that is, *Ctns*$^{-/-}$, *Ctns*$^{-/-}$ *Il6*$^{-/-}$, *Ctns*$^{-/-}$ *Il1β*$^{-/-}$, and WT mice. All mice were 12 months old and were fed *ad libitum*. The study period was 6 weeks. Food intake and weight gain in mice were compared (*E* and *F*). For the third study, we investigated the metabolic effects of genetic deletion of *Il6* and *Il1β* in *Ctns*$^{-/-}$ mice beyond nutritional stimulation by employing a pair-feeding approach. Specifically, *Ctns*$^{-/-}$ mice were fed *ad libitum* for 6 weeks while *Ctns*$^{-/-}$ *Il6*$^{-/-}$, *Ctns*$^{-/-}$ *Il1β*$^{-/-}$, and WT mice were pair-fed to that of *Ctns*$^{-/-}$ mice (*G*). Weight gain, fat and lean content, 24 h oxygen consumption, left gastrocnemius wet weight, and *in vivo* muscle function (rotarod and grip strength) were measured in mice (*H–N*). Results of second and third studies were expressed as mean ± SEM. Results of *Ctns*$^{-/-}$, *Ctns*$^{-/-}$ *Il6*$^{-/-}$, and *Ctns*$^{-/-}$ *Il1β*$^{-/-}$ were compared with WT mice significance represented by $^{\#}$. In addition, results of *Ctns*$^{-/-}$ *Il6*$^{-/-}$ and *Ctns*$^{-/-}$ *Il1β*$^{-/-}$ mice were also compared with *Ctns*$^{-/-}$ mice, respectively (*E–N*), and statistical significance (*P* value) is shown above bar.

(EchoMRI-100™, Echo Medical System) twice, prior to the initiation of the study as well as at the end of the study, and change of total body fat and lean mass in individual mouse was calculated. Twenty-four-hour metabolic rate (VO_2) of mice was measured using Oxymax indirect calorimetry (Columbus Instrument) at the end of the study. At the end of the study, muscle function (grip strength and rotarod activity) in mice was assessed using a grip strength metre (Model 47106, UGO Basile) and rotarod performance tool (model RRF/SP, Accuscan Instrument), respectively.[9,11]

Protein assay for muscle and adipose tissue

Mice were sacrificed at the end of the study, and gastrocnemius muscle, inguinal white adipose tissue (WAT), and intercapsular brown adipose tissue were dissected and processed in a homogenizer tube (USA Scientific, catalogue 1420-9600) containing ceramic beads (Omni International, catalogue 19-646) using a Bead Mill Homogenizer (Omni International). Protein concentration of tissue homogenate was assayed using Pierce BAC Protein Assay Kit (Thermo Scientific, catalogue 23227). Uncoupling protein (UCP) content and adenosine triphosphate (ATP) concentration in adipose tissue and muscle homogenates were assayed. Protein concentration of phospho-ERK 1/2 (Thr202/Ty2r204) and total ERK 1/2, phospho-JNK (The183/Tyr185) and total JNK, phospho-p38 MAPK (Thr180/Tyr182) and total p38 MAPK, NF-κB p65 (phospho-Ser536) and total NF-κB p65, and IL-6 and IL-1β in muscle homogenates was assayed (*Table* S1).

Gastrocnemius wet weight, fiber size, and fatty infiltration

The left gastrocnemius muscle of mice was dissected at the end of the study. Wet weight of the left gastrocnemius muscle was recorded immediately after tissue excision and utilized for subsequent protein and mRNA studies. Freshly excised right gastrocnemius muscle was frozen in isopentane/liquid nitrogen and stored in −80°C before further processing. Muscle cryosections were used for muscle

DOI: 10.1002/jcsm.12744

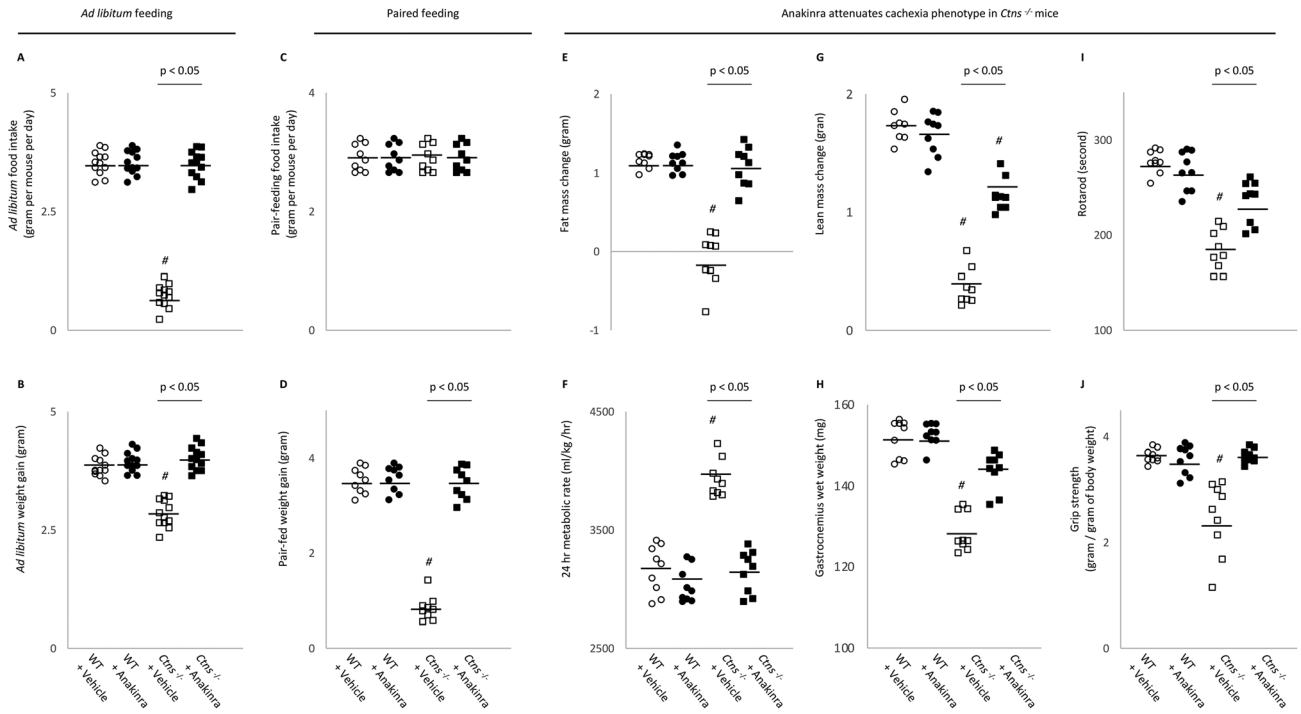

Figure 2 Anakinra attenuates cachexia in *Ctns*$^{-/-}$ mice. Twelve-month-old WT and *Ctns*$^{-/-}$ mice were treated with anakinra (2.5 mg/kg/day, IP) or normal saline as a vehicle control for 6 weeks. All mice were fed *ad libitum* for 6 weeks, and food intake and weight were recorded (*A* and *B*). In another experiment, to assess the beneficial effects of anakinra beyond its nutritional effects, we employed a pair-feeding strategy. Vehicle-treated *Ctns*$^{-/-}$ mice were given an *ad libitum* amount of food whereas other groups of mice were given an equivalent amount of food (*C*). Weight gain, fat and lean content, 24 h oxygen consumption, left gastrocnemius wet weight, and *in vivo* muscle function (rotarod and grip strength) were measured in the mice (*D–J*). Data are expressed as mean ± SEM. Results of vehicle-treated *Ctns*$^{-/-}$ mice were compared with vehicle-treated WT mice while results of anakinra-treated *Ctns*$^{-/-}$ mice were compared with that of anakinra-treated WT mice ($^{\#}P < 0.05$). In addition, results of anakinra-treated *Ctns*$^{-/-}$ mice were compared with vehicle-treated *Ctns*$^{-/-}$ mice, and specific *P* value is shown above bar.

fiber cross-sectional area assessment as well as Oil Red O staining. We measured muscle fiber cross-sectional area of gastrocnemius muscle, using ImageJ software (https://rsbweb.nih.gob/ij/).[9,11] In addition, portions of the dissected right gastrocnemius muscle samples were incubated with Oil Red O (Oil Red O Solution, catalogue number O0625, Sigma Aldrich). Detailed procedures for Oil Red O staining were in accordance with published protocol.[12] We followed a recently established protocol to quantify muscle fat infiltration. Acquisition and quantification of images were analysed using ImageJ software.[13]

Muscle RNAseq analysis

Previously, we performed RNAseq analysis on gastrocnemius muscle mRNA in 12-month-old *Ctns*$^{-/-}$ mice versus age-appropriate WT mice.[11] Detailed procedures for mRNA extraction, purification, and subsequent construction of cDNA libraries as well as analysis of gene expression were published. We then performed Ingenuity Pathway Analysis enrichment tests for those differentially expressed muscle genes in *Ctns*$^{-/-}$ mice versus WT mice, focusing on pathways related to energy metabolism, skeletal and muscle system development and function, and organismal injury and abnormalities. We identified the top 20 differentially expressed muscle genes in *Ctns*$^{-/-}$ versus WT mice.[11] In this study, we performed qPCR analysis for those top 20 differentially expressed gastrocnemius muscle genes in the different experimental groups.

Quantitative real-time PCR

Total RNA from adipose and gastrocnemius muscle samples was isolated using TriZol (Life Technology) and reverse transcribed with SuperScript III Reverse Transcriptase (Invitrogen). Quantitative real-time RT-PCR of target genes was performed using KAPA SYBR FAST qPCR kit (KAPA Biosystems). Expression levels were calculated according to the relative $2^{-\Delta\Delta Ct}$ method.[11] All primers are listed (*Table* S2).

DOI: 10.1002/jcsm.12744

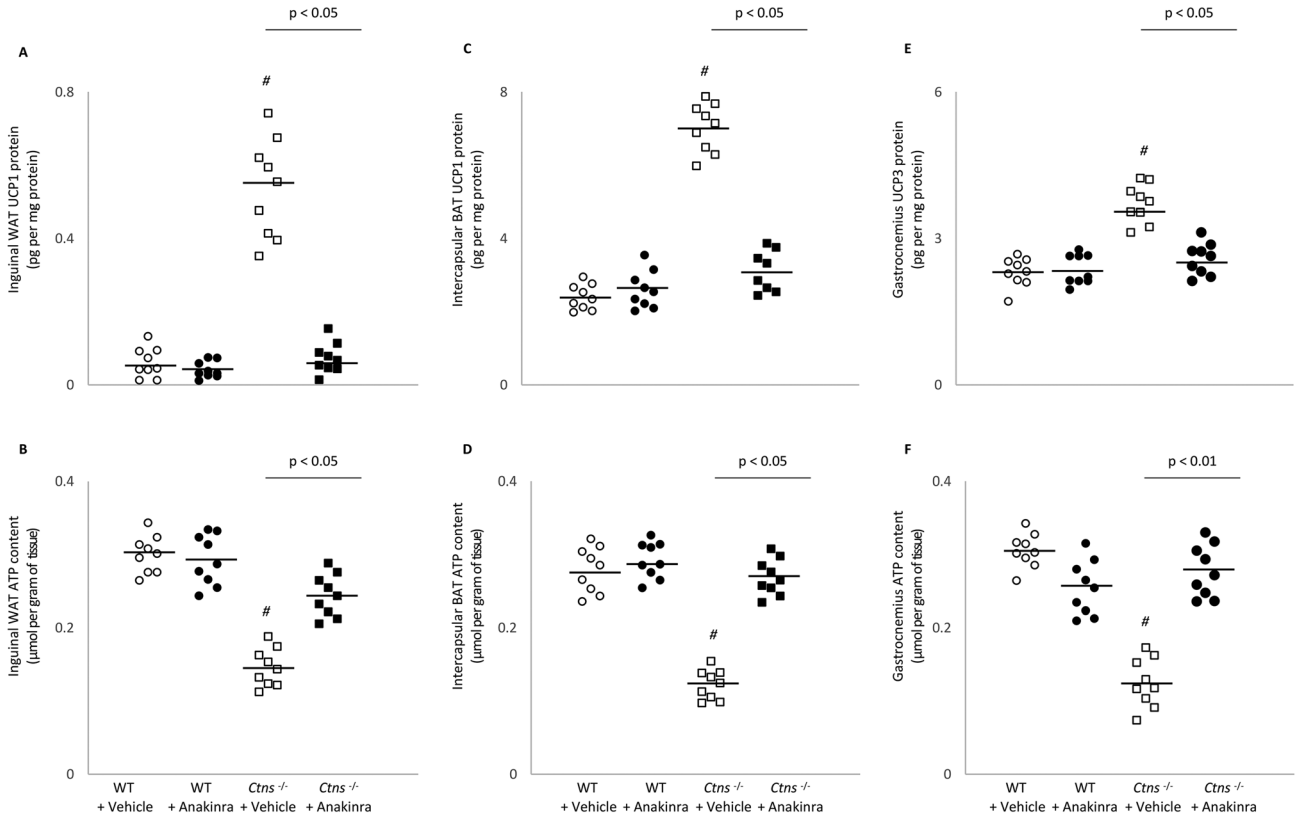

Figure 3 Anakinra ameliorates energy homeostasis in adipose tissue and skeletal in *Ctns*$^{-/-}$ mice. UCPs and ATP content in adipose tissue (inguinal white adipose tissue and brown adipose tissue) and gastrocnemius muscle were measured. Results are analysed and expressed as in *Figure* 2.

Statistical analysis

Continuous variables are expressed as mean ± standard error of the mean. We assessed the statistical significance of differences between groups using two-sample *t*-tests. All tests were two-sided. A *P* value less than 0.05 was considered significant. Statistical analyses were performed using SPSS software Version 16.0 for Macintosh. # represents a statistically significant ($P < 0.05$) difference from WT control mice. Bars with specific *P* values between groups represent a statistical significance from *Ctns*$^{-/-}$ mice.

Results

Increased muscle interleukin-6 and interleukin-1β mRNA and protein content in Ctns$^{-/-}$ *mice*

We chose to study *Ctns*$^{-/-}$ mice at 12 months of age based on our previous data demonstrating a significant cachexia phenotype. As expected, all of the mice were uraemic and had elevated creatine, but normal bicarbonate levels serum (*Table* S3). In order to investigate the role of inflammatory cytokines in cachexia and muscle wasting, we measured gastrocnemius muscle mRNA and protein content of IL-6 and IL-1β in 12-month-old *Ctns*$^{-/-}$ mice and age-matched WT controls. Gastrocnemius mRNA and protein content of both IL-6 and IL-1β were significantly elevated in *Ctns*$^{-/-}$ mice relative to WT mice (*Figure* 1A–1D).

Genetic deletion of Il1β normalizes cachexia in Ctns$^{-/-}$ *mice*

We then employed a genetic approach to determine whether *IL6* and *I1β* deficiency would affect the cachexia phenotype in *Ctns*$^{-/-}$ mice. Twelve-month-old *Ctns*$^{-/-}$, *Ctns*$^{-/-}$ *Il6*$^{-/-}$, and *Ctns*$^{-/-}$ *Il1β*$^{-/-}$ mice were all uraemic and had elevated creatinine levels but normal bicarbonate levels (*Table* S4). All mice were fed *ad libitum* for 6 weeks, and average daily food intake and final weight gain of the mice were recorded. We showed that genetic deletion of *Il1β* completely corrected anorexia and normalized weight gain in *Ctns*$^{-/-}$ mice whereas deletion of *Il6* only partially rescued the phenotype in *Ctns*$^{-/-}$ mice (*Figure* 1E and 1F). Furthermore, to investigate the potential metabolic effects of genetic deficiency of *Il1β* and *Il6* beyond its nutritional effects, we employed a pair-feeding strategy. *Ctns*$^{-/-}$ mice were fed *ad libitum*, and

DOI: 10.1002/jcsm.12744

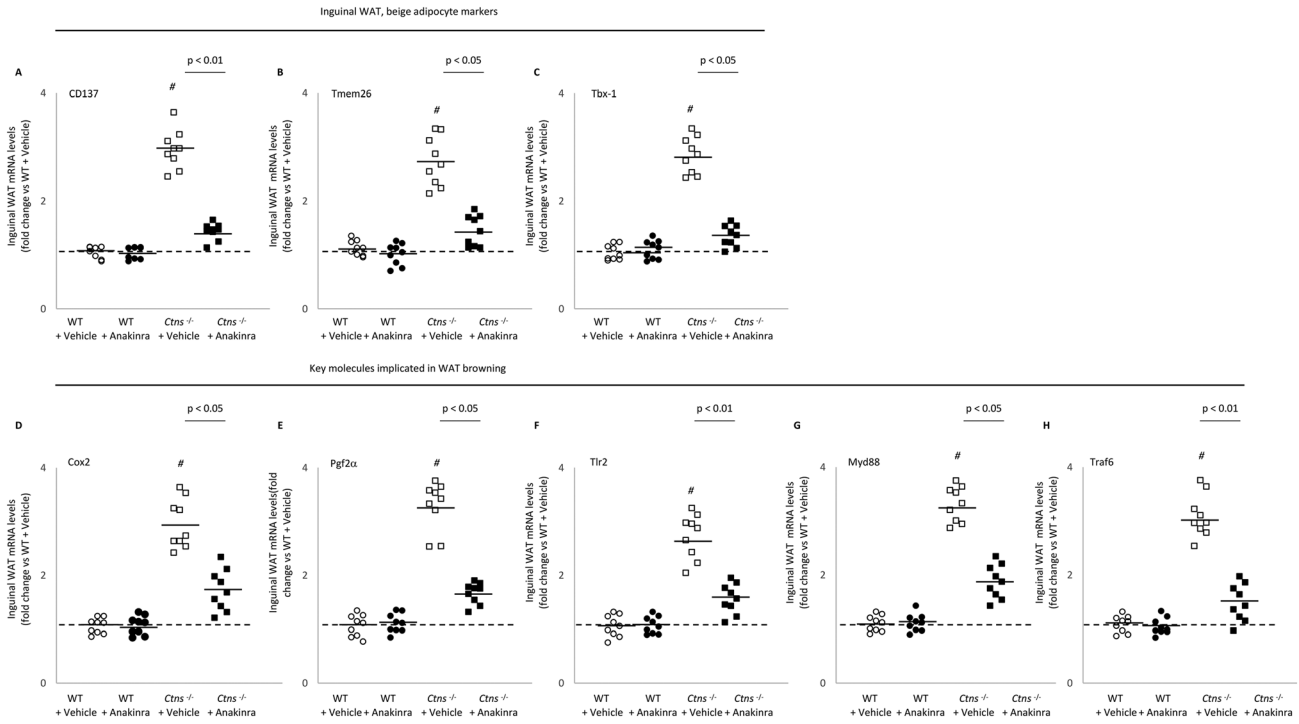

Figure 4 Anakinra attenuates adipose tissue browning in *Ctns*$^{-/-}$ mice. Gene expression of beige adipocyte markers (CD137, Tmem26, and Tbx-1) in inguinal white adipose tissue was measured. Gene expression of Cox2 signalling pathway (Cox2 and Pgf2α) and toll-like receptor pathway (Tlr2 and MyD88) in inguinal white adipose tissue was also measured. Gene expression was measured by qPCR. Final results were expressed in arbitrary units, with one unit being the mean level in vehicle-treated WT mice. Results are analysed and expressed as in *Figure* 2.

then all other groups of mice were fed the same amount of rodent diet based on the recorded food intake of the *Ctns*$^{-/-}$ group (*Figure* 1G). Despite receiving the same amount of total calorie intake as other groups of mice, cardinal features of cachexia phenotype such as decreased weight gain, decreased fat mass content and hypermetabolism (manifested as elevated oxygen consumption), decreased lean mass content and gastrocnemius weight, and reduced muscle function (decreased rotarod and grip strength) were still prominent in *Ctns*$^{-/-}$ mice (*Figure* 1H–1N). Importantly, parameters of cachexia phenotype were normalized relative to WT mice or significantly improved in *Ctns*$^{-/-}$ *Il1β*$^{-/-}$ mice compared with *Ctns*$^{-/-}$ mice. However, *Ctns*$^{-/-}$ *Il6*$^{-/-}$ mice had only minimal non-significant improvement relative to *Ctns*$^{-/-}$ mice.

Anakinra attenuates cachexia and muscle wasting in Ctns$^{-/-}$ *mice*

In order to better model a real-world approach in patients, we used a pharmacological approach to test the effects of IL-1β blockade in pre-established INC-associated cachexia and muscle wasting. Anakinra, an IL-1 receptor antagonist that blocks both IL-1α and IL-1β function, was used to treat 12-month-old *Ctns*$^{-/-}$ mice and WT controls for 6 weeks compared with vehicle. All mice were fed *ad libitum*. Food intake and weight gain were normalized in anakinra-treated *Ctns*$^{-/-}$ mice (*Figure* 2A and 2B). We also investigated the beneficial effects of anakinra in *Ctns*$^{-/-}$ mice beyond appetite stimulation and its consequent body weight gain through the utilization of a pair-feeding approach. Daily *ad libitum* food intake for *Ctns*$^{-/-}$ mice treated with vehicle was recorded. Following that, anakinra-treated *Ctns*$^{-/-}$ mice and WT mice treated with anakinra or vehicle were food restricted such that the mice ate an equivalent amount of food as vehicle-treated *Ctns*$^{-/-}$ mice (*Figure* 2C). Serum and blood chemistry of mice were measured (*Table* S5). Anakinra normalized weight gain, and metabolic rate and significantly improved or normalized fat and lean mass content, gastrocnemius weight, and muscle function (grip strength and rotarod activity) in *Ctns*$^{-/-}$ mice (*Figure* 2D–2J).

Anakinra normalizes energy homeostasis in adipose tissue and skeletal muscle in Ctns$^{-/-}$ *mice*

Adipose tissue (inguinal WAT and intercapsular brown adipose tissue) and gastrocnemius protein content of UCPs was significantly increased in *Ctns*$^{-/-}$ mice compared with

DOI: 10.1002/jcsm.12744

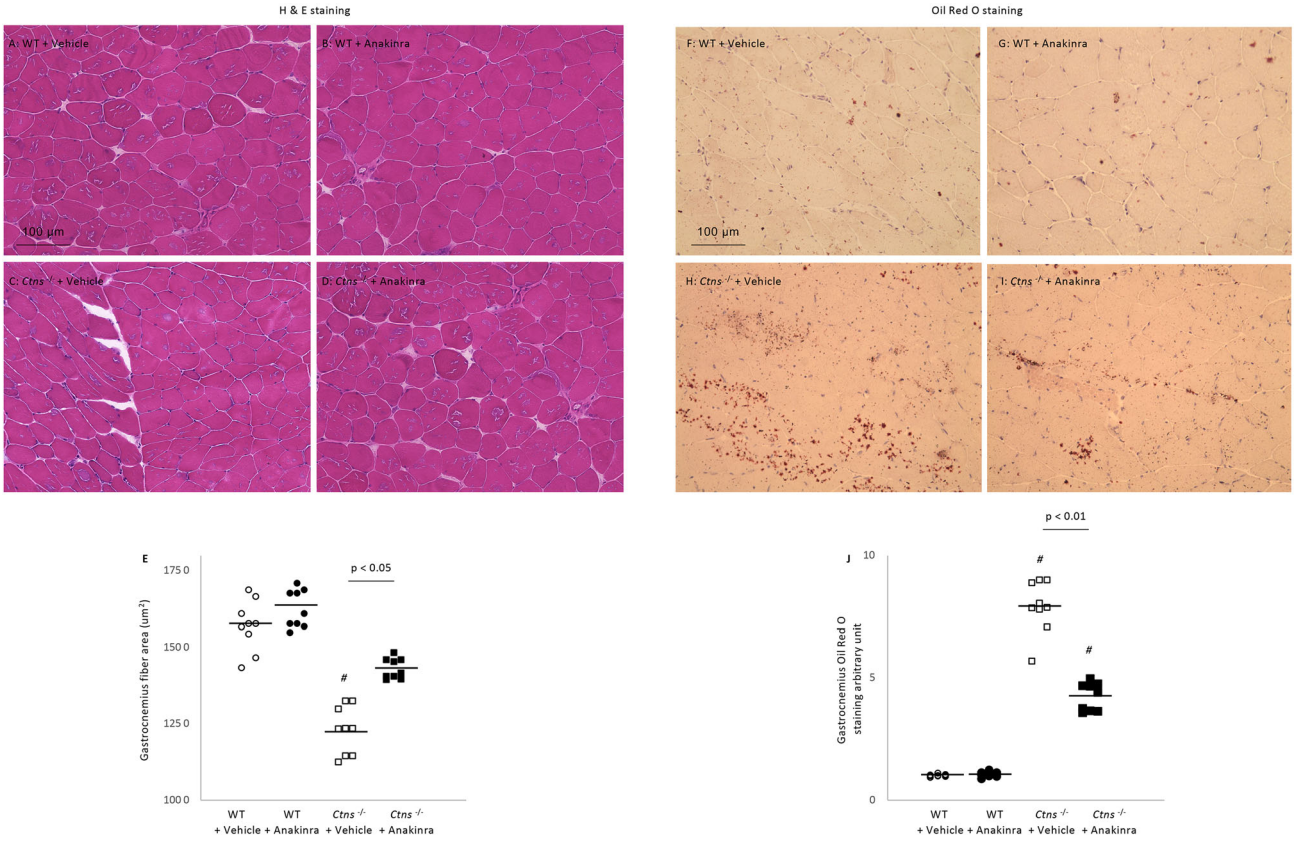

Figure 5 Anakinra normalizes muscle fiber size and attenuates muscle fat infiltration in *Ctns*$^{-/-}$ mice. Representative photomicrographs of gastrocnemius with H&E staining (*A–D*). Average gastrocnemius cross-sectional area was measured (*E*). Visualization of quantification of fatty infiltration by Oil Red O analysis in gastrocnemius muscle (*F–J*). Final results were expressed in arbitrary units, with one unit being the mean staining intensity in vehicle-treated WT mice. Difference among various groups of mice was analysed as in *Figure* 2.

WT mice (*Figure* 3A, 3C, and 3E). In contrast, ATP content in adipose tissue and skeletal muscle was significantly decreased in *Ctns*$^{-/-}$ mice compared with WT mice (*Figure* 3B, 3D, and 3F). Anakinra normalized UCPs and ATP content of adipose tissue and muscle in *Ctns*$^{-/-}$ mice.

Anakinra ameliorates browning of adipose tissue in Ctns$^{-/-}$ *mice*

Beige adipose cell surface markers (CD137, Tmem26, and Tbx1) mRNA levels were elevated in inguinal WAT in *Ctns*$^{-/-}$ mice relative to WT mice (*Figure* 4A–4C). This was accompanied by an increased UCP-1 protein content in inguinal WAT shown in *Figure* 3A, which is a biomarker for beige adipocytes, and usually undetectable in WAT. Anakinra normalized the elevated protein content of inguinal WAT UCP-1 as well as increased mRNA expression of CD137, Tmen, and Tbx1 in *Ctns*$^{-/-}$ mice (Figures 3A and 4A–4C). Anakinra also ameliorated expression of important signature molecules implicated in WAT. Activation of the Cox2/Pgf2α signalling pathway and chronic inflammation stimulate biogenesis of WAT browning. Significantly increased inguinal WAT mRNA expression of Cox2 and Pgf2α was found in *Ctns*$^{-/-}$ mice compared with WT mice (*Figure* 4D and 4E). Moreover, inguinal WAT levels of toll-like receptor 2 (Tlr2) as well as myeloid differentiation primary response 88 (MyD88) and tumour necrosis factor receptor-associated factor 6 (Traf6) were up-regulated in *Ctns*$^{-/-}$ mice compared with WT mice (*Figure* 4F–4H), and anakinra significantly reduced inguinal WAT gene expression of Cox2/Pgf2α as well as genes in the toll-like receptor pathway in *Ctns*$^{-/-}$ mice.

Anakinra improves muscle fiber size and attenuates muscle fat infiltration in Ctns$^{-/-}$ *mice*

We evaluated the effect of anakinra on skeletal muscle morphology in *Ctns*$^{-/-}$ mice. Representative results of muscle sections are illustrated (*Figure* 5A–5D). Anakinra significantly improved average cross-sectional area of gastrocnemius fibers in *Ctns*$^{-/-}$ mice (*Figure* 5E). We also evaluated fat

DOI: 10.1002/jcsm.12744

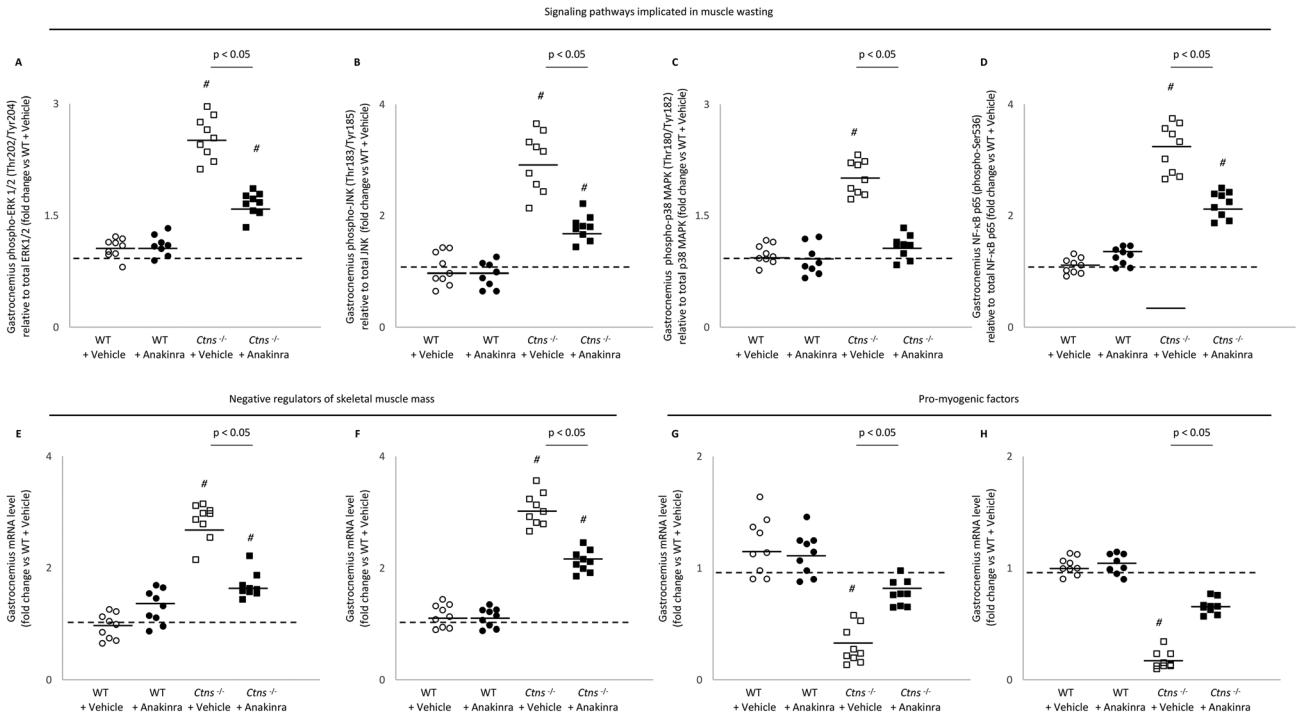

Figure 6 Anakinra attenuates signalling pathways implicated in muscle wasting in *Ctns*$^{-/-}$ mice. Gastrocnemius muscle relative phospho-Akt (pS473)/total Akt ratio, relative phospho-ERK 1/2 (Thr202/Tyr204)/total ERK 1/2 ratio, relative phospho-JNK (Thr183/Tyr185)/total JNK ratio, relative phospho-p38 MAPK (Thr180/Tyr182)/total p38 MAPK, and relative phosphorylated NF-κB p65 (Ser536)/total p65 ratio as well as relative phosphor Ικκα (Ser536)/total Ικκα ratio in mice. In addition, gastrocnemius muscle expression of interested genes was measured by qPCR. Final results were expressed in arbitrary units, with one unit being the mean level in vehicle-treated WT mice. Results are analysed and expressed as in *Figure* 2.

infiltration of the gastrocnemius muscle in *Ctns*$^{-/-}$ mice. Representative results of Oil Red O staining of muscle section are shown (*Figure* 5F–5I). We quantified intensity of muscle fat infiltration in mice and observed that anakinra attenuated muscle fat infiltration in *Ctns*$^{-/-}$ mice (*Figure* 5J).

Anakinra attenuates signalling pathways implicated in muscle wasting in Ctns$^{-/-}$ *mice*

Muscle relative phospho-ERK 1/2 (Thr202/Tyr204), phospho-JNK (Thr183/Tyr185), and phospho-p38 MAPK protein content (Thr180/Tyr182) were significantly increased in *Ctns*$^{-/-}$ mice compared with WT mice (*Figure* 6A–6C). In addition, the ratio of muscle phospho-NF-κB p65 (phosphorylated S536) relative to total NF-κB p65 protein content was elevated in *Ctns*$^{-/-}$ mice relative to WT mice (*Figure* 6D). Importantly, anakinra attenuated or normalized phosphorylation of muscle ERK 1/2, JNK, p38 MAPK, and NF-κB p65 protein content in *Ctns*$^{-/-}$ mice. Administration of anakinra improved muscle regeneration and myogenesis by decreasing mRNA expression of negative regulators of skeletal muscle mass (Atrogin-1 and Myostatin) (*Figure* 6E and 6F) as well as increasing muscle mRNA expression of pro-myogenic factors (MyoD and Myogenin) in *Ctns*$^{-/-}$ mice (*Figure* 6G and 6H).

Molecular mechanism by RNAseq analysis

Recently, we profiled differential expression of gastrocnemius mRNA between 12-month-old *Ctns*$^{-/-}$ mice and WT mice using RNAseq analysis.[11] Ingenuity Pathway Analysis enrichment tests identified the top 20 differentially expressed muscle genes in *Ctns*$^{-/-}$ mice versus WT mice. The top 15 up-regulated genes were Ankdr2, Csrp3, Cyfip2, Fhl1, Ly6a, Mup1, Myl2, Myl3, Nlrc3, Sell, Sln, Spp1, Tnnc1, Tnni1, and Tpm3 whereas the top 5 down-regulated genes were Atf3, Cidea, Fos, Sncg, and Tbc1d1 in *Ctns*$^{-/-}$ mice relative to WT mice. We performed qPCR analysis for those top 20 differentially expressed muscle genes in the present study. Importantly, anakinra significantly reduced (Ankdr2, Csrp3, Cyfip2, Fhl1, Ly6a, Nlrc3, Tnnc1, and Tpm3) and significantly increased (Atf3, Cidea, Sncg, and Tbc1d1) muscle gene expression in *Ctns*$^{-/-}$ mice relative to WT mice (*Figures* S1 and S2). Functional significance of each of these 12 genes is listed (*Table* 1). Non-significant changes were observed in Mup1, Myl2, Myl3, Sell, Sln, Spp1, Tnni1, and Fos.

DOI: 10.1002/jcsm.12744

Table 1 Anakinra normalized or attenuated expression of important muscle genes that have been implicated in muscle wasting in *Ctns*$^{-/-}$ mice

Up-regulated DEG	Functional significance and reference
Ankrd2	Implicated in mechanical stretch of skeletal muscle[14,15]
Csrp3	Associated with skeletal muscle dystrophy[16]
Cyfip2	Associated with muscle wasting[17]
Fhl1	Activates myostatin signalling and promotes atrophy in skeletal muscle[18]
Ly6a	Associated with remodelling of the extracellular matrix during skeletal muscle regeneration[19]
Nlrc3	Implicated in skeletal muscle wasting by inhibiting cell proliferation and promoting cell apoptosis[20]
Tnnc1	Regulates striated muscle contraction[21] Implicated in cardiomyopathy pathogenesis and age-related skeletal muscle wasting[21]
Tpm3	Promotes slow myofibre hypotrophy and associated with generalized muscle weakness[22]
Down-regulated DEG	**Functional significance**
Atf3	Impairs motor neuron survival and muscle innervation[23]
Cidea	Increases metabolic rates, lipolysis in brown adipose tissue, and higher core temperature[24]
Sncg	Increases energy expenditure, particularly in brown and white adipose tissues[25] Associated with cancer cachexia through the TGF-β signalling pathway[25]
Tbc1d1	Impairs glucose transport in skeletal muscle[26] Associated with follistatin-induced muscle hypertrophy[26]

Previously, we studied differential expression of gastrocnemius mRNA between *Ctns*$^{-/-}$ mice and WT mice using RNAseq analysis.[11] We focus on pathways related to energy metabolism, skeletal and muscular system development and function, nervous system development and function, and organismal injury and abnormalities. In the present study, we performed qPCR analysis for top 20 differentially expressed muscle genes determined by our previous studies. Importantly, anakinra normalized (Ankdr2, Csrp3, Ly6a, Nlrc3, Tnnc1 and Tpm3, Atf3, Cidea, Sncg, and Tbc1d1) and attenuated (Cyfip2 and Fhl1) muscle gene expression in *Ctns*$^{-/-}$ mice relative to WT mice. Functional significance of each of these differentially expressed muscle genes is listed. DEG, differential expressed genes.

Discussion

Previously, we described cachexia characterized by adipose tissue browning and muscle wasting in *Ctns*$^{-/-}$ mice, an established mouse model of INC, but the aetiology was not clear. Increased expression of inflammatory cytokines such as IL-6 and IL-1 have been implicated in the aetiology of cachexia and muscle. Our studies using specific cytokine-deficient mice and IL-1 targeted therapy suggest that IL-1 is a critical cytokine in INC-associated cachexia. The novel findings of this study are (i) anakinra corrects anorexia, normalizes weight gain, and attenuates hypermetabolism. (ii) Anakinra attenuates the expression of markers of adipose tissue browning as well as perturbed energy expenditure and thermogenesis. (iii) Anakinra attenuates muscle wasting, improved muscle function, and corrected perturbations of aberrant expression of molecules implicated in muscle wasting. Together, our results suggest that anakinra may be an effective targeted treatment approach for cachexia in patients with INC.

Interleukin-1β suppresses food intake, activates energy metabolism, and reduces weight gain in experimental animals.[27,28] IL-1β signals through appetite-regulating neuropeptides, such as leptin resulting in appetite suppression.[29] We have demonstrated that elevated circulating level of leptin through the activation of melanocortin receptor 4 induces CKD-associated cachexia.[30] IL-1 and IL-6 are produced not only by circulating immune cells but also by various cells in tissues such as muscle and adipose tissue. For this present study, we showed that skeletal muscle IL-1β and IL-6 mRNA and protein level was significantly increased in *Ctns*$^{-/-}$ mice, and *Ctns*$^{-/-}$ *Il1β*$^{-/-}$ mice had normalized parameters of cachexia phenotype relative to control mice (*Figure* 1). Furthermore, we showed that anakinra improved anorexia and normalized weight gain in *Ctns*$^{-/-}$ mice relative to control mice (*Figure* 2). Our results further highlight the beneficial effects of anakinra beyond food stimulation and accompanied weight gain. In pair-fed studies in which anakinra-treated *Ctns*$^{-/-}$ mice and anakinra-treated WT mice were fed the same amount of food, cachexia was attenuated in anakinra-treated *Ctns*$^{-/-}$ mice relative to control mice (*Figure* 2).

The basal metabolic rate accounts for up to 80% of the daily calorie expenditure by individual.[31] Skeletal muscle metabolism is a major determinant of resting energy expenditure.[32,33] IL-1β increases basal metabolic rate (as represented by an increase in resting oxygen consumption) in a dose-dependent manner.[34] In our study, anakinra normalized the increased 24 h metabolic rate in *Ctns*$^{-/-}$ mice (*Figure* 2F). Adipose tissue UCP-1 expression is essential for adaptive adrenergic non-shivering thermogenesis, and muscle UCP-3 level controls body metabolism.[35] The energy generated when dissipating the proton gradient via up-regulation of UCPs is not used for cellular ATP production or other biochemical processes but instead to produce heat.[36,37] We showed that anakinra normalized muscle and adipose tissue UCPs and ATP content in *Ctns*$^{-/-}$ mice (*Figure* 3). Blockade of IL-1 receptor signalling may also mitigate the metabolic dysfunction through leptin signalling. Infusion of leptin increased UCPs expression in skeletal muscle and adipose tissue.[38,39]

DOI: 10.1002/jcsm.12744

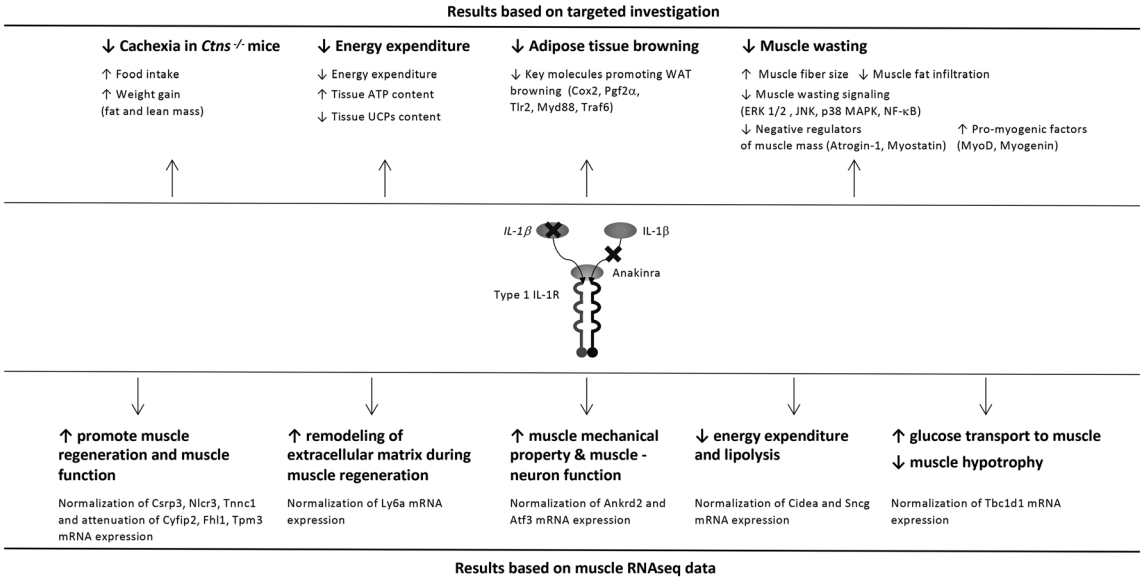

Figure 7 Summary of the beneficial effects of anakinra on cachexia, energy homeostasis, adipose tissue browning, and muscle wasting in *Ctns*$^{-/-}$ mice.

Perhaps our most novel finding is that anakinra reduced adipose tissue browning in *Ctns*$^{-/-}$ mice. New evidence suggests a maladaptive role of adipose tissue browning in the context of cachexia.[40] Activation of adipose tissue browning is associated with profound energy expenditure and weight loss in cachectic patients. Browning of adipose tissue increases energy expenditure and takes place before skeletal muscle atrophy in murine models of cancer and CKD-associated muscle wasting.[41,42] We previously demonstrated adipose tissue browning in *Ctns*$^{-/-}$ mice (as evidenced by the detection of inguinal WAT UCP-1 protein and increased expression of beige adipose cell markers CD137, Tmem, and Tbx1).[9,11] Cox2 is a downstream effector of β-adrenergic signalling and induces biogenesis of beige cells in WAT depots.[43] We showed that anakinra normalized expression of inguinal WAT Cox2, Pgf2α, and important inflammatory molecules (Tlr2, MyD88, and Trap6) in *Ctns*$^{-/-}$ mice and normalized key inflammatory molecules (Tlr2 and MyD88) involved in adipose tissue browning in *Ctns*$^{-/-}$ mice (*Figure* 4). Recent data suggest that IL1β signalling mediates adipocyte browning via regulating of mitochondrial oxidative responses in both cultured human and animal adipocytes.[44]

We studied the impact of anakinra on muscle wasting in *Ctns*$^{-/-}$ mice. Anakinra normalized lean mass content, gastrocnemius wet weight, and muscle function in *Ctns*$^{-/-}$ mice relative to WT mice (*Figure* 2G–2J). Furthermore, anakinra normalized average gastrocnemius cross-sectional area as well as muscle fat infiltration of gastrocnemius muscle in *Ctns*$^{-/-}$ mice (*Figure* 5). Muscle fat infiltration is a significant predictor of both muscle function and mobility function across a wide variety of co-morbid conditions such as diabetes, spinal cord injury, and kidney disease.[45–47] Muscle adipose tissue may release pro-inflammatory cytokines within the muscle and impair the local muscle environment, impair blood flow, or increase the rate of lipolysis within skeletal muscle resulting in an increased concentration of glucose within the skeletal muscle itself followed by insulin resistance.[48,49]

We investigated the impact of anakinra on signalling molecules that modulate muscle mass regulation in *Ctns*$^{-/-}$ mice. Systemic inflammation decreases muscle regeneration and increases muscle catabolism that eventually leads to muscle wasting in CKD. Inhibition of IL-1 reduced systemic inflammation (decreased serum CRP and IL-6) in CKD patients.[8,50] A recent study also showed that blockade of IL-1 signalling significantly improved inflammatory status (a decrease in plasma concentration of IL-6 and TNF) and antioxidative properties in CKD patients.[51] Systemic inflammation, as assessed by serum concentration of CRP, is a strong and independent risk factor for skeletal muscle wasting in CKD patients.[52] IL-1 has been shown to stimulate the expression of catabolic genes.[6,53,54] MAPK are a family of protein phosphorylating enzymes that regulate a diverse aspect of cellular responses including skeletal muscle regeneration and differentiation.[55–57] Activation of the NF-κB signalling pathway leads to severe muscle wasting in mice.[58] IL-1α and IL-1β, both isoforms of IL-1, stimulated catabolism in C2C12 myotubes via activation of NF-κB signalling and atrogin-1 expression.[4] Importantly, anakinra attenuated or normalized phosphorylation of muscle ERK 1/2, JNK, p38 MAPK, and NF-κB p65 protein content in *Ctns*$^{-/-}$ mice. In addition, anakinra improved muscle regeneration and myogenesis by decreasing mRNA expression of negative regulators of skeletal muscle mass (Atrogin-1 and Myostatin)

DOI: 10.1002/jcsm.12744

as well as increasing muscle mRNA expression of pro-myogenic factors (MyoD and Myogenin) in *Ctns*$^{-/-}$ mice (*Figure* 6). Our findings were in agreement with a recent report demonstrating that IL-1β administration inhibiting muscle mRNA expression of atrogin-1.[27]

Finally, we studied the impact of anakinra on muscle transcriptomics in *Ctns*$^{-/-}$ mice. We showed that anakinra normalized or attenuated muscle expression of 12 out of 20 top differentially expressed genes in *Ctns*$^{-/-}$ mice.[11] Detailed functional significance of each of these 12 differentiated expressed muscle genes is listed in *Table* 1. Anakinra normalized (Csrp3, Ly6a, Nlrc3, Tnnc1 and Tpm3, Atf3, Cidea, Sncg, and Tbc1d1) and attenuated (Cyfip2 and Fhl1) muscle gene expression in *Ctns*$^{-/-}$ mice relative to WT mice (*Figures* S1 and S2). Increased expression of Csrp3, Cyfip2, Fhl1, Nlcr3, Tnnc1, and Tpm3 have been implicated in muscle atrophy and muscle weakness.[16–18,20–22] Increased expression of Ly6a has been associated with aberrant remodelling of the extracellular matrix during skeletal muscle regeneration.[19] In addition, increased expression of Ankrd2 as well as decreased expression of Atf3 impairs muscle function and impairs survival of motor neuron and muscle innervation.[14,15,23] Recent data also suggest that decreased expression of Cidea and Sncg are associated with higher energy expenditure as well as accelerated lipolysis of adipose tissue.[24,25] Furthermore, decreased expression of Tbc1d1 impairs glucose transport in skeletal muscle and has been implicated in follistatin-induced muscle hypertrophy.[26]

Conclusion

We employed genetic and pharmacological approaches and demonstrated significant beneficial effects of IL-1 blockade on cachexia in *Ctns*$^{-/-}$ mice. We report that anakinra attenuates adipose tissue browning and muscle wasting in *Ctns*$^{-/-}$ via multiple cellular mechanisms (*Figure* 7). IL-1 receptor antagonist may represent a novel targeted treatment for cachexia in patients with INC by attenuating adipose tissue browning and muscle wasting.

Acknowledgements

All authors of this manuscript certify that they complied with the ethical guidelines for authorship and publishing in the *Journal of Cachexia, Sarcopenia and Muscle* update 2017.[59]

Conflict of interest

None declared.

Funding

This investigation was supported by National Institutes of Health (RO1 DK12581). This investigation was also supported in whole or in part by a grant from the Cystinosis Research Foundation. R.M. is funded by grants from the NIH (RO1 DK125811, R01 HD095547, U01 DK066143) and the California Institute of Regenerative Medicine (CLIN2-11478). H.H. is funded by NIH awards R01 DK113592, R01 HL140898, R01 AI134030 and a UC collaborative grant. P.Z. was supported by 'Spring Sunlight Program' cooperative research project of Ministry of Education (HLJ2019023) and Research Fund for Young & Middle-Aged Innovative Science of the Second Affiliated Hospital of Harbin Medical University (CX2016-03).

Online supplementary material

Additional supporting information may be found online in the Supporting Information section at the end of the article.

Table S1: Immunoassay information for blood and serum chemistry, muscle adenosine triphosphate content as well as muscle and adipose tissue protein analysis.
Table S2: PCR primer information.
Table S3: Serum and blood chemistry of 12-month old *Ctns*$^{-/-}$ and wild type control mice. Data are expressed as mean ± SEM. Result of serum chemistry of *Ctns*$^{-/-}$ mice were compared to WT mice. # $p < 0.05$, significantly increased in *Ctns*$^{-/-}$ mice relative to WT mice.
Table S4: Serum and blood chemistry of *Ctns*$^{-/-}$, *Ctns*$^{-/-}$ *Il6*$^{-/-}$, *Ctns*$^{-/-}$*Il1*b$^{-/-}$ and wild type control mice. Experiment was 6 weeks. Data are expressed as mean ± SEM. Result of *Ctns*$^{-/-}$—, *Ctns*$^{-/-}$*Il6*$^{-/-}$ and *Ctns*$^{-/-}$*Il1*b$^{-/-}$ mice were compared to WT mice. # $p < 0.05$, significantly increased in *Ctns*$^{-/-}$, *Ctns*$^{-/-}$*Il6*$^{-/-}$ and *Ctns*$^{-/-}$*Il1*b$^{-/-}$ mice relative to WT mice.
Table S5: Serum and blood chemistry of *Ctns*$^{-/-}$ and wild type control mice. Twelve-month old WT and *Ctns*$^{-/-}$ mice were treated with anakinra (2.5 mg.kg per day, IP) or vehicle (normal saline) for 6 weeks. Vehicle treated *Ctns*$^{-/-}$ mice were fed *ad libitum* while other group of mice were pair-fed with the same amount of rodent diet as consumed by vehicle treated *Ctns*$^{-/-}$ mice. Result of serum chemistry of *Ctns*$^{-/-}$ + Vehicle mice were compared to WT + Vehicle mice while results of *Ctns*$^{-/-}$ + Anakinra mice were compared to WT + Anakinra mice. Data are expressed as mean ± SEM. # $p < 0.05$, significantly increased in *Ctns*$^{-/-}$ + Vehicle and *Ctns*$^{-/-}$ + Anakinra relative to WT + Vehicle and WT + Anakinra mice, respectively.

Figure S1: Anakinra attenuates upregulated signature molecules implicated in $Ctns^{-/-}$ associated muscle wasting and cachexia. Gastrocnemius muscle expression of interested genes in mice was measured by qPCR. Final results were expressed in arbitrary units, with one unit being the mean level in vehicle-treated WT mice. Data are expressed as mean ± SEM. Results of vehicle-treated $Ctns^{-/-}$ mice were compared to vehicle-treated WT mice while results of anakinra-treated $Ctns^{-/-}$ mice were compared to that of anakinra-treated WT mice. In addition, results of anakinra-treated $Ctns^{-/-}$ mice were compared to vehicle-treated $Ctns^{-/-}$ mice. # $p < 0.05$.

Figure S2: Anakinra attenuates downregulated signature molecules implicated in *$Ctns^{-/-}$* associated muscle wasting and cachexia. Gastrocnemius muscle expression of interested genes in mice was measured by qPCR. Final results were expressed in arbitrary units, with one unit being the mean level in vehicle-treated WT mice. Data are expressed and analysed as supplemental figure 1.

References

1. Nesterova G, Gahl W. Nephropathic cystinosis: late complications of a multisystemic disease. *Pediatr Nephrol* 2008;**23**:863–878.
2. Theodoropoulos DS, Krasnewich D, Kaiser-Kupfer MI, Gahl WA. Classic nephropathic cystinosis as an adult disease. *JAMA* 1993;**270**:2200–2204.
3. Prencipe G, Caiello I, Cherqui S, Whisenant T, Petrini S, Emma F, et al. Inflammasome activation by cystine crystals: implications for the pathogenesis of cystinosis. *J Am Soc Nephrol* 2014;**25**:1163–1169.
4. Li W, Moylan JS, Chambers MA, Smith J, Reid MB. Interleukin-1 stimulates catabolism in C2C12 myotubes. *Am J Physiol Cell Physiol* 2009;**297**:C706–C714.
5. Huang N, Kny M, Riediger F, Busch K, Schmidt S, Luft FC, et al. Deletion of Nlrp3 protects from inflammation-induced skeletal, muscle atrophy. *Intensive Care Med Exp* 2017;**5**:3.
6. Dinarello CA. Overview of the IL-1 family in innate inflammation and acquired immunity. *Immunol Rev* 2018;**281**:8–27.
7. Klimek MEB, Sali A, Rayavarapu S, Van der Meulen JH, Nagaraju K. Effect of the IL-1 receptor antagonist Kineret on disease phenotype in mdx mice. *PLos ONE* 2016; **11**:e0155944.
8. Hung AM, Ellis CD, Shintani A, Booker C, Ikizler TA. IL-1β receptor antagonist reduces inflammation in hemodialysis patients. *J Am Soc Nephrol* 2011;**22**:437–442.
9. Cheung W, Cherqui S, Ding W, Esparza W, Zhou P, Shao J, et al. Muscle wasting and adipose tissue browning in infantile nephropathic cystinosis. *J Cachexia Sarcopenia Muscle* 2016;**7**:152–164.
10. Young S, Struys E, Wood T. Quantification of creatinine and guanidinoacetate using GC-MS and LC-MS/MS for the detection of cerebral creatinine deficiency syndromes. *Curr Protoc Hum Genet* 2007; 17.3.1–17.3.18.
11. Cheung W, Hao S, Wang Z, Ding W, Zheng R, Gonzalez A, et al. Vitamin D repletion ameliorates adipose tissue browning and muscle wasting in infantile nephropathic cystinosis. *J Cachexia Sarcopenia Muscle* 2020;**11**:120–134.
12. Dubowitz V. Histological and histochemical stains and reactions. In Dubowitz V et al., eds. *Muscle Biopsy. A Practical Approach*, 4th ed. Amsterdam: Elsevier; 2013.
13. Mehlem A, Hagberg CE, Kuhl L, Eriksson U, Falkwvall A. Imaging of neutral lipids by oil red O for analyzing the metabolic status in health and disease. *Nat Protoc* 2013;**8**: 1149–1154.
14. Kemp TJ, Sadusky TJ, Saltisi F, Carey N, Moss J, Yang SY, et al. Identification of Ankrd2, a novel skeletal muscle gene coding for a stretch-response ankyrin-repeat protein. *Genomics* 2000;**66**:229–241.
15. Mohamed JS, Lopez MA, Cox GA, Boriek AM. Anisotropic regulation of Ankrd2 gene expression in skeletal muscle by mechanical stretch. *FASEB J* 2010;**24**: 3330–3340.
16. Cui C, Han S, Tang S, He H, Shen X, Zhao J, et al. The autophagy regulatory molecules CSRP3 interacts with LC3 and protects against muscular dystrophy. *Int J Mol Sci* 2020;**21**:749.
17. Llano-Diex M, Gustafson AM, Olsson C, Goransson H, Larsson L. Muscle wasting and the temporal gene expression pattern in a novel rat intensive care unit model. *BMC Genomics* 2011;**12**:602.
18. Lee JY, Lori D, Wells DJ, Kemp PR. FHL1 activates myostatin signaling in skeletal muscle and promotes atrophy. *FEBS Open Bio* 2015;**5**:753–762.
19. Kafadar KA, Yi L, Ahmad Y, So L, Rossi F, Pavlath GK. Sca-1 expression is required for efficient remodeling of the extracellular matrix during skeletal muscle regeneration. *Dev Bio* 2009;**326**:47–59.
20. Karki R, Malireddi RKS, Zhu Q, Kanneganti TD. NLRC3 regulates cellular proliferation and apoptosis to attenuate the development of colorectal cancer. *Cell Cycle* 2017;**16**:1243–1251.
21. Johnson JR, Chase PB, Ointo JR. Troponin through the looking-glass: emerging roles beyond regulation of straited muscle contraction. *Oncotarget* 2018;**9**:1461–1482.
22. Yuen M, Cooper ST, Marston SB, Nowak KJ, McNamara E, Mokbel N, et al. Muscle weakness in TPM3-myopathy is due to reduced Ca^{2+}-sensitivity and impaired actomyosin cross-bridge cycling in slow fibres. *Hum Mol Genet* 2015;**24**:6278–6292.
23. Shijffers R, Zhang J, Matthews JC, Chen A, Tamrazian E, Babaniyi O, et al. Atf3 expression improves motor function in the ALS mouse model by promoting motor neuron survival and retaining muscle innervation. *Proc Natl Acad Sci U S A* 2014;**111**: 1622–1627.
24. Abreu-Vieira G, Fischer AW, Mattsson C, de Jong JM, Shabalina IG, Ryden M, et al. Cidea improves the metabolic profile through expansion of adipose tissue. *Nat Commun* 2015;**6**:7433.
25. Shao T, Song P, Hua H, Zhang H, Sun X, Kong X, et al. Gamma synuclein is a novel Twist1 target that promotes TGF-β-induced cancer cell migration and invasion. *Cell Death Dis* 2018;**9**:625.
26. Han X, Moller LLV, Groote ED, Bojsen-Moller KN, Davey J, Henriquez-Olguin CH, et al. Mechanisms involved in follistatin-induced hypertrophy and increase insulin action in skeletal muscle. *J Cachexia Sarcopenia Muscle* 2019;**10**: 1241–1257.
27. Braun TP, Zhu X, Szumowski M, Scott GD, Grossberg AJ, Levasseur PR, et al. Central nervous system inflammation induces muscle atrophy via activation of the hypothalamic–pituitary–adrenal axis. *J Exp Med* 2011;**208**:2449–2463.
28. Tocco-Bradley R, Georgieff M, Jones CT, Moldawer LL, Dinarello CA, Blackburn GL, et al. Changes in energy expenditure and fat metabolism in rats infused with interleukin-1. *Eur J Clin Invest* 1987;**17**:504–510.
29. Sachot C, Poole S, Luheshi GN. Circulating leptin mediates lipopolysaccharide-induced anorexia and fever in rats. *J Physiol* 2004;**561**:263–272.
30. Cheung W, Yu PX, Little BM, Cone RD, Marks DL, Mak RH. Role of leptin and melanocortin signaling in uremia-associated cachexia. *J Clin Invest* 2005;**115**:1659–1665.
31. Eckel-Mahan K, Sassone-Corsi P. Metabolism and the circadian clock converge. *Physiol Rev* 2013;**93**:107–135.
32. van den Berg SA, van Marken LW, Willems van Dijk K, Schrauwen P. Skeletal muscle mitochondrial uncoupling, adaptive thermogenesis and energy expenditure. *Curr Opin Clin Nutr Metab Care* 2011;**14**: 243–249.
33. Zurlo F, Larson K, Bogardus C, Ravussin E. Skeletal muscle metabolism is a major

DOI: 10.1002/jcsm.12744

determinant of resting energy expenditure. *J Clin Invest* 1990;**86**:1423–1427.
34. Dascombe MJ, Rothwell NJ, Sagay BO, Stock MJ. Pyrogenic and thermogenic effects of interleukin 1 beta in the rat. *Am J Physiol* 1989;**256**:E7–E11.
35. Rousset S, Alves-Guerra MC, Mozo J, Miroux B, Cassard-Doulcier AM, Bouillaud F, et al. The biology of mitochondrial uncoupling proteins. *Diabetes* 2004;**53**: S130–S135.
36. Argiles JM, Busquets S, Lopez-Sorian FJ. The role of uncoupling proteins in pathophysiological states. *Biochem Biophy Res Commun* 2002;**293**:1145–1152.
37. Sluse FE. Uncoupling proteins: molecular, functional, regulatory, physiological and pathological aspects. *Adv Exp Med Biol* 2012;**942**:137–156.
38. Rouru J, Cusin I, Zakrzewska KE, Jeanrenaud B, Rohner-Jeanrenaud F. Effects of intravenously infused leptin on insulin sensitivity and on the expression of uncoupling proteins in brown adipose tissue. *Endocrinology* 1999;**140**:3688–3692.
39. Tajima D, Masaki T, Hidaka S, Kakuma T, Sakata T, Yoshimatsu H. Acute central infusion of leptin modulates fatty acid mobilization by affecting lipolysis and mRNA expression for uncoupling proteins. *Exp Biol Med (Maywood)* 2005;**230**:200–206.
40. Kir S, White J, Kleiner S, Kazak L, Cohen P, Baracos VE, et al. Tumour-derived PTH related protein triggers adipose tissue browning and cancer cachexia. *Nature* 2014;**513**:100–104.
41. Petruzzelli M, Wagner EF. Mechanisms of metabolic dysfunction in cancer cachexia. *Genes Dev* 2016;**30**:489–501.
42. Kir S, Komaba H, Garcia AP, Economopoulos KP, Liu W, Lanske B, et al. PTH/PTHrP receptor mediates cachexia in models of kidney failure and cancer. *Cell Metab* 2016;**23**:315–323.
43. Vegiopoulos A, Müller-Decker K, Strzoda D, Schmitt I, Chicheknitskiy E, Ostertag A, et al. Cyclooxygenase-2 controls energy homeostasis in mice by de novo recruitment of brown adipocytes. *Science* 2010;**328**: 1158–1161.
44. Okla M, Zaher W, Alfayez M, Chung S. Inhibitory effects of Toll-like receptor 4, NLRP3 Inflammasome, and interleukin-1β on white adipocyte browning. *Inflammation* 2018;**41**:626–642.
45. Addison O, Marcus RL, LaStayo PC, Yuan AS. Intermuscular fat: a review of the consequences and causes. *Int J Endocrino* 2014;Article ID: 309570.
46. Goodpaster BH, Thaete FL, Kelley DE. Thigh adipose tissue distribution is associated with insulin resistance in obesity and in type 2 diabetes mellitus. *Am J Clin Nutr* 2000;**71**:885–892.
47. Cheema B, Abas H, Smith B, O'Sullivan AJ, Chan M, Patwardhan A, et al. Investigation of skeletal muscle quality and quality in end-stage renal disease. *Nephrology (Carlton)* 2010;**15**:454–463.
48. Beasley LE, Koster A, Newman AB, Javaid MK, Ferrucci L, Kritchevsky SB, et al. Inflammation and race and gender differences in computerized tomography-measured adipose depots. *Obesity* 2009;**17**:1062–1069.
49. Sam S, Haffner S, Davidson MH, D'Agonstino RB, Feinstein S, Kondos G, et al. Relation of abdominal fat depots to systemic markers of inflammation in type 2 diabetes. *Diabetes Care* 2009;**32**: 932–937.
50. Nowak KL, Chonchol M, Ikizler TA, Farmer-Bailey H, Salas N, Chaudhry R, et al. IL-1 inhibition and vascular function in CKD. *J Am Soc Nephrol* 2017;**28**:971–980.
51. Hung AM, Tsuchida Y, Nowak KL, Sarkar S, Chonchol M, Whitfield V, et al. IL-1 inhibition and function of the HDL-containing fraction of plasma in patients with stages 3 to 5 CKD. *Clin J Am Soc Nephrol* 2019;**14**:702–711.
52. Deger SM, Hung AM, Gamboa JL, Siew ED, Ellis CD, Booker C, et al. Systemic inflammation is associated with exaggerated skeletal muscle protein catabolism in maintenance hemodialysis patients. *JCI Insight* 2017;**2**:e95185.
53. Londhe P, Guttridge DC. Inflammation induced loss of skeletal muscle. *Bone* 2014;**80**:131–142.
54. Ballak DB, Stienstra R, Tack CJ, Dinarello CA, van Diepen JA. IL-1 family members in the pathogenesis and treatment of metabolic disease: focus on adipose tissue inflammation and insulin resistance. *Cytokine* 2015;**75**:280–290.
55. Geisler HWS, Shi H, Gerrard DE. MAPK pathway in skeletal muscle diseases. *J Vet Anim Husb* 2013;**1**:e104.
56. Zetser A, Gredinger E, Bengal E. p38 mitogen-activated protein kinase pathway promotes skeletal muscle differentiation. Participation of the Mef2c transcription factor. *J Biol Chem* 1999;**274**: 5193–5200.
57. Wu Z, Woodring PJ, Bhakta KS, Tamura K, Wen F, Feramisco JR, et al. p38 and extracellular signal-regulated kinases regulate the myogenic program at multiple steps. *Mol Cell Biol* 2000;**20**:3951–3964.
58. Cai D, Frantz JD, Tawa NE Jr, Melendez PA, Oh BC, Lidov HG, et al. IKKbeta/NF-kappaB activation causes severe muscle wasting in mice. *Cell* 2004;**119**:285–298.
59. von Haehling S, Morley JE, Coats AJS, Anker SD. Ethical guidelines for publishing in the *Journal of Cachexia, Sarcopenia and Muscle*: update 2017. *J Cachexia Sarcopenia Muscle* 2019;**10**:1143–1145.